THE ASTROPHYSICAL JOURNAL, 430:L33–L36, 1994 July 20

THE TRUE NUCLEUS OF NGC 253 REVEALED BY HIGH-RESOLUTION NEAR-INFRARED IMAGING

BRUCE J. SAMS, III, R. GENZEL, A. ECKART, L. TACCONI-GARMAN, AND R. HOFMANN
Max-Planck-Institut für Extraterrestrische Physik, Giessenbachstraße, D-85748 Garching, Germany
Received 1993 August 9; accepted 1994 March 7

ABSTRACT

The nucleus of starburst galaxy NGC 253 has been located with high resolution *J*-, *H*-, *K*-band imaging. It lies shrouded in a dense dust cloud with $A_V \gtrsim 24$ and molecular mass $\approx 6 \times 10^4\ M_\odot$ located $\approx 2\farcs2$ northwest of the intensity peak in the *J*, *H*, and *K* maps. The nucleus is identified with the brightest 6 cm radio point source. The intensity peak itself has substantial emission from hot gas of at least 500 K. The other "hot spots" are merely holes in the dust, rather than intrinsically luminous areas. A dense structure of molecular gas of mass $5 \times 10^4\ M_\odot$ extends ≈ 70 pc along the major axis. This structure shows evidence of curvature consistent with spiral arms. The molecular material/dust in the bar traces the 6 cm radio continuum emission. Dense knots of molecular gas are correlated with 6 cm radio peaks, suggesting that the fainter radio sources are H II regions rather than supernovae or supernova remnants.

Subject headings: galaxies: individual (NGC 253) — galaxies: nuclei — infrared: galaxies — stars: formation — supernovae: general

1. INTRODUCTION

In this *Letter* we present new sub-arcsecond resolution near-infrared (NIR) observations of the prototypical starburst galaxy NGC 253 which clarify the structure and emission mechanisms of the central 150 pc starburst region. NGC 253 lies 2.5 Mpc distant and is inclined at the nearly edge-on angle of 78°, which increases the observed dust extinction toward the starburst. The starburst region is highly gas enriched, with an H_2/H I column density 10 times higher than in the disk (Combes, Gottesman, & Weliachew 1977; Scoville et al. 1985). Such a density implies that many molecular clouds have fallen inward from the disk, possibly induced to do so by the 3 kpc bar detected at 2.2 μm (Scoville et al. 1985), as there is neither an inner Lindblad resonance (Telesco, Dressel, & Wolsencroft 1993) nor a merger interaction to drive gas inward (Olson & Kwan 1990). At least some of this gas is quite dense and warm [$n(H_2) \approx 10^4$ cm^{-3}, $T \gtrsim 50$ K], as shown by the ^{12}CO $J = 6 \rightarrow 5$ emission peak within 10″ of the nucleus (Harris et al. 1991). The total far-infrared luminosity of $\approx 3 \times 10^{10}\ L_\odot$ (Telesco & Harper 1980) requires an ionizing flux equivalent to 1000 O6 stars within the central 150 pc (Turner & Ho 1985), which in turn implies O star–formation rates of $\gtrsim 1.6\ M_\odot$ yr^{-1} and supernova rates of ≈ 0.05 yr^{-1} (Forbes et al. 1993). NIR images show bright "hot spots" in the starburst region, which Forbes and collaborators (Forbes, Ward, & DePoy 1991; Forbes et al. 1993) have interpreted as star-formation centers. The proposed galactic nucleus is a powerful flat spectrum radio source with characteristics similar to other compact synchrotron sources in active galaxies and quasars (Turner & Ho 1985). There is also a large family of less luminous radio point sources with spectra of variable steepness extending roughly 40″ along a line passing through the proposed nucleus (Antonucci & Ulvestaad 1988; Ulvestaad & Antonucci 1991). Despite the depth and breadth of knowledge about NGC 253, several important questions about its starburst region remain unanswered. The precise nature and position of the IR nucleus itself, for example, is still unclear, as are the heating mechanisms of the dust/molecular material and the nature of the less luminous radio point sources. This *Letter* addresses those questions.

2. OBSERVATIONS AND DATA REDUCTION

We observed NGC 253 on 1992 August 16 using the MPE NIR camera SHARP (Hofmann et al. 1993) at the New Technology Telescope (NTT) of the European Southern Observatory (ESO). SHARP can capture and store images as fast as 3 Hz, with individual frame times as short as 50 ms. This permits several kinds of high-resolution processing, including rapid guidance (Ribak 1986) and speckle imaging (Roddier 1988). With 256 × 256 pixels and a pixel scale of $0\farcs05$ pixel^{-1}, our $12\farcs8$ square field of view covered essentially all of the central ≈10″ starburst region. Wide-band filters at *J* (1.2 μm), *H* (1.6 μm), and *K* (2.2 μm) provided color discrimination. Each data set consists of 100 frames each of 5 s exposure. Selected frames (≈90 per data set) were then co-added using a simple shift-and-add (SSA) algorithm (see, e.g., Christou 1991), with the brightest point in the IR maps as a reference source. This produced images with a fundamental spatial resolution of FWHM $0\farcs7$. Using the image of a similarly processed and well-sampled reference star (SAO 166596) as a point-spread function reference, we sharpened these images from $0\farcs7$ to $0\farcs5$ resolution using a Lucy algorithm (Lucy 1974). The Lucy algorithm is flux conserving, and we have found through experience that its results are very reliable. Our photometric reference was 9 Sgr, which was assumed to have magnitudes of 5.83 (*J*), 5.85 (*H*), and 5.84 (*K*) (Koorneef 1985). Our absolute flux calibration error is ≲10%.

3. RESULTS AND DISCUSSION

3.1. *NIR and Extinction Morphologies: Interpreting the Maps*

Figures 1 and 2 show the $0\farcs5$ (6 pc) resolution *J*- and *K*-band maps in contour form. The *J* map shows more structure and with greater intensity variation than the *K* map, suggesting that the perceived brightness distribution is dominated by patchy dust extinction rather than by varying intrinsic source colors. There are many local intensity maxima—"hot

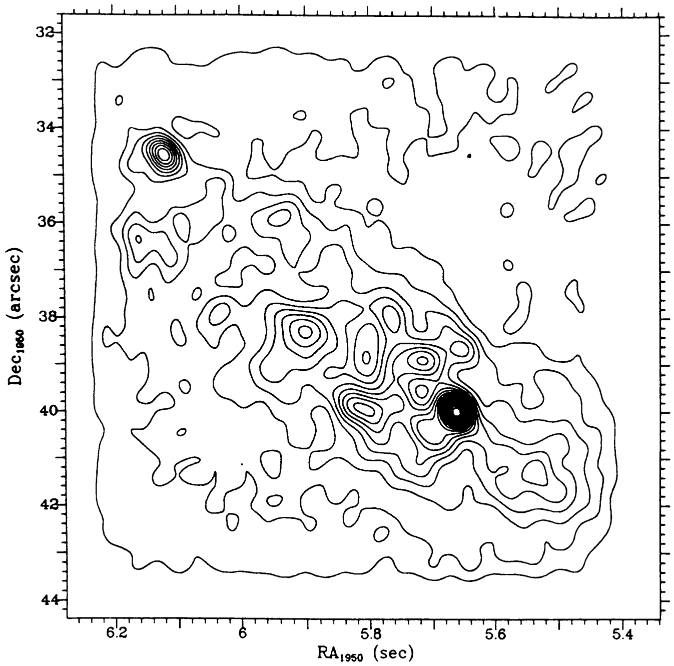

FIG. 1.—*J*-band contour map of NGC 253 with effective resolution of 0ʺ.5. Contour levels are 10, 15, 20, 25, 30, 35, 40, 45, 50, 60, 70, 80, 90, 100% of peak. Right ascension must be prefixed with 00^h45^m, declination with $-25°33'$. The astrometric positions of all maps are those derived by placing the intensity maximum at its mean position as determined from other measurements (see text). In this case the absolute position of the proposed radio nucleus (known to $\lesssim 0''.1$) falls within 0ʺ.1 of the point we call the nucleus.

spots"—visible in both maps, 15 of which are shown labeled in the *J*-band false color image of Figure 3 (Plate L1). The relative alignment of the *J*-, *H*-, and *K*-band images (checked by global cross-correlation) is $\leq 0''.1$. All three bands are dominated by the same NIR intensity maximum. Figure 4 (Plate L2) shows the absolute calibrated $J-K$ image with overlays of the 6 cm radio continuum contours and point sources (Antonucci & Ulvestaad 1988). The map shows a central peak of high extinction connected to a long thin structure along the major axis. Also evident in the map is an overall extinction level with a gradient of $J-K \approx 0.1$ mag arcsec^{-1}, such that the northwestern edge is the more heavily extincted.

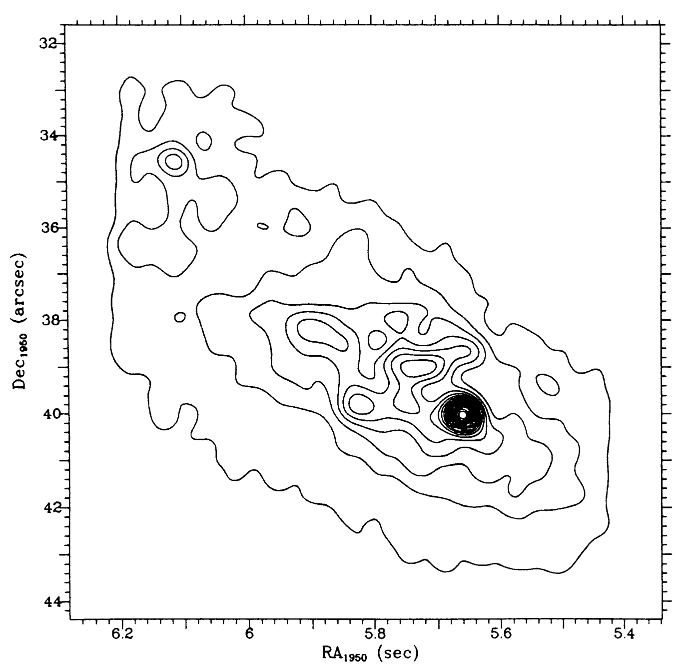

FIG. 2.—*K*-band contour map of NGC 253. Contour levels at 10, 15, 20, 25, 30, 35, 40, 45, 50, 60, 70, 80, 90, 100% of peak. Right ascension must be prefixed with 00^h45^m, declination with $-25°33'$.

3.2. *The "Hot Spots" Are Not Hot*

Forbes and collaborators (Forbes et al. 1991; Forbes et al. 1993) have seen two of the brighter "hot spots" visible in our images and interpreted them as compact circumnuclear star-formation regions (our spots *g* and *f* are their spots *A* and *B* in the 1993 paper). We investigated the nature of the spots by flux counting in a 0ʺ.5 diameter aperture centered on each of them. The fluxes were calibrated in magnitudes, and the derived $J-H$ and $H-K$ values plotted (see Fig. 5) to indicate the relative importance of dust extinction on the perceived colors. The simplest explanation of nearly all the spot colors is that they are due to a patchy ($A_V \approx 1$–5) veil of dust which unevenly obscures the surface brightness of the smooth galactic distribution behind it. *Thus, the "hot spots" are not "hot" at all; they are an artifact of uneven extinction.*

Only three spots are inconsistent (to within our errors) with this pure extinction hypothesis, namely spots *e*, *m*, and the NIR peak, all of whose colors can be explained by a mixture of pure extinction and some intrinsic emission due to hot dust (Glass & Moorwood 1985). An extinction of $A_V \approx 4$ mixed with $\approx 30\%$ emission from dust at 500 K would move the NIR peak to its observed position, while only 10% dust emission would suffice in the cases of spots *e* and *m*. What is heating this dust/molecular material? We checked the possibility of supernova heating by looking for time variability in the NIR peak's flux. Using a high-quality *H*-band array image from 1985 (Rieke, Lebofsky, & Walker 1988) for comparison, we found no flux variation within our 20% (combined) calibration errors.

3.3. *Identification of the Galactic Nucleus*

Recently Piña, Jones, & Puetter (1992) determined that the NIR intensity maximum is not the galactic nucleus. Based on astrometrical comparisons with published maps, they associate a secondary peak of 10.7 μm emission (their IRS 2) with the radio nucleus. We have performed a similar analysis by aligning our maps with two published maps of known position. This produced two position estimates for the NIR intensity peak; the weighted mean of these estimates is our preferred NIR peak position. Our first reference is an *H*-band map with a final absolute positional accuracy of 1ʺ.5 obtained by reference to a 10 μm absolute position measurement (Rieke et al. 1988; Reike 1993). We reconvolved our high-resolution *H*-band map to the spatial resolution of the reference *H* image and then matched the positions of the intensity peak to obtain an absolute position of $\alpha = 00^h45^m05^s.70$, $\delta = -25°33'40''.0$ (1950) for the NIR intensity peak. Our second reference is a 10.8 μm map with positional accuracy of 1ʺ.5 (Telesco et al. 1993). We convolved our *K*-band map to the 4ʺ resolution of the 10.8 μm map and then compared the overall contours of the maps. Despite their wavelength difference, the degraded resolution *K*-band and 10.8 μm maps can be aligned to within 0ʺ.5 by a two-dimensional cross-correlation. In this way we determine the position of our *K*-band intensity peak to be $\alpha = 00^h45^m05^s.63$, $\delta = -23°33'40''.2$ to an error of $\sqrt{1.5^2 + 0.5^2} = 1''.6$. The correlation between bands is accept-

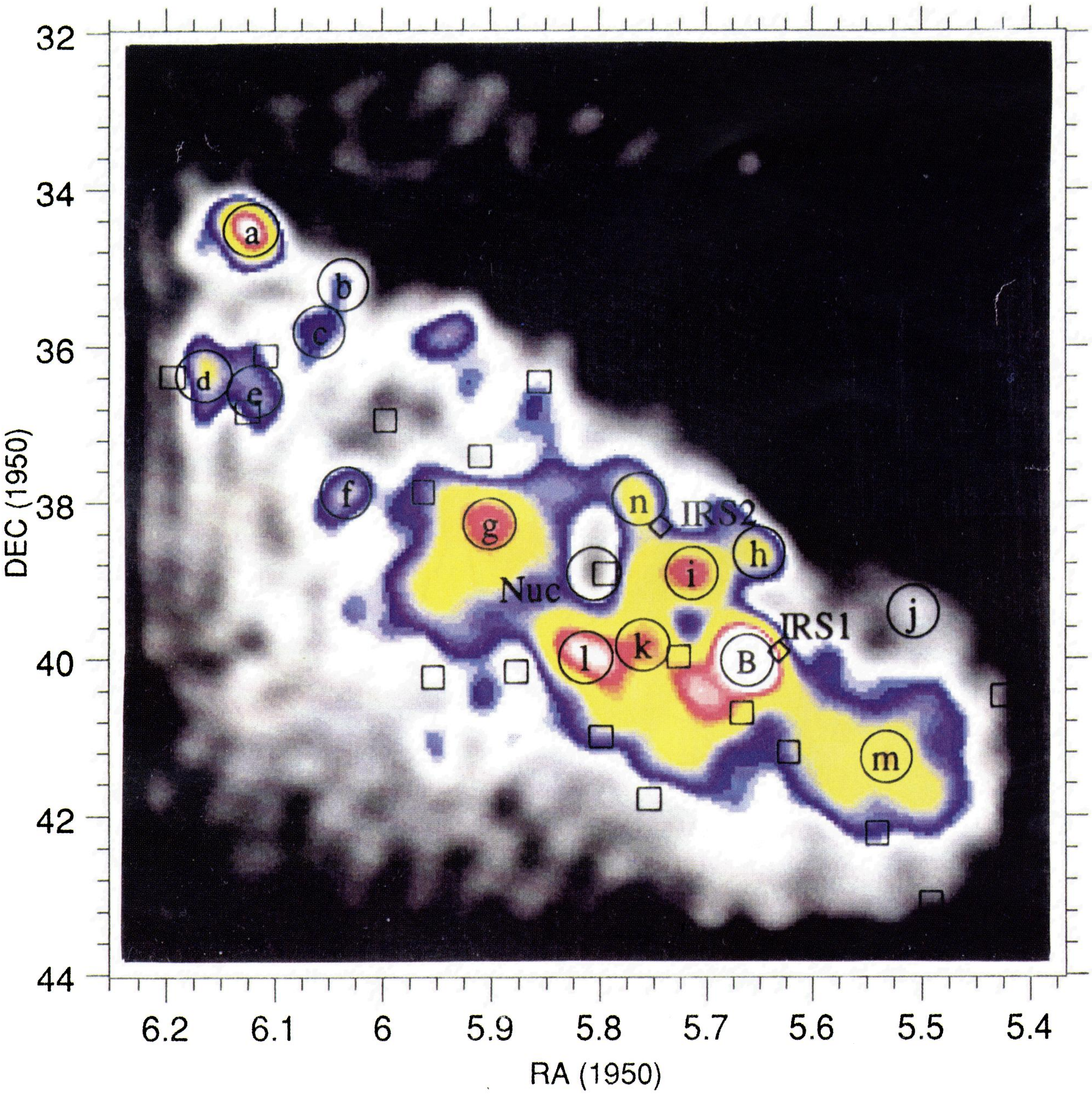

FIG. 3.—*J*-band image of NGC 253. Circles and letters mark the positions and names of intensity maxima visible in all three of the *J*-, *H*-, and *K*-band images. The NIR maximum is marked with a "B." The effective image resolution is 0ʺ.5 (the size of the circles), and the brightness scale is logarithmic. Small squares mark positions of 6 cm radio peaks (Ulvestaad & Antonuuci 1991). The square corresponding to the proposed radio nucleus is labeled. The nucleus itself appears as a dark region rather than as an intensity peak in this image, because it is hidden behind $A_V \gtrsim 20$ of dust. Right ascension must be prefixed with 00^h45^m, declination with $-25°33'$.

SAMS et al. (see 430, L34)

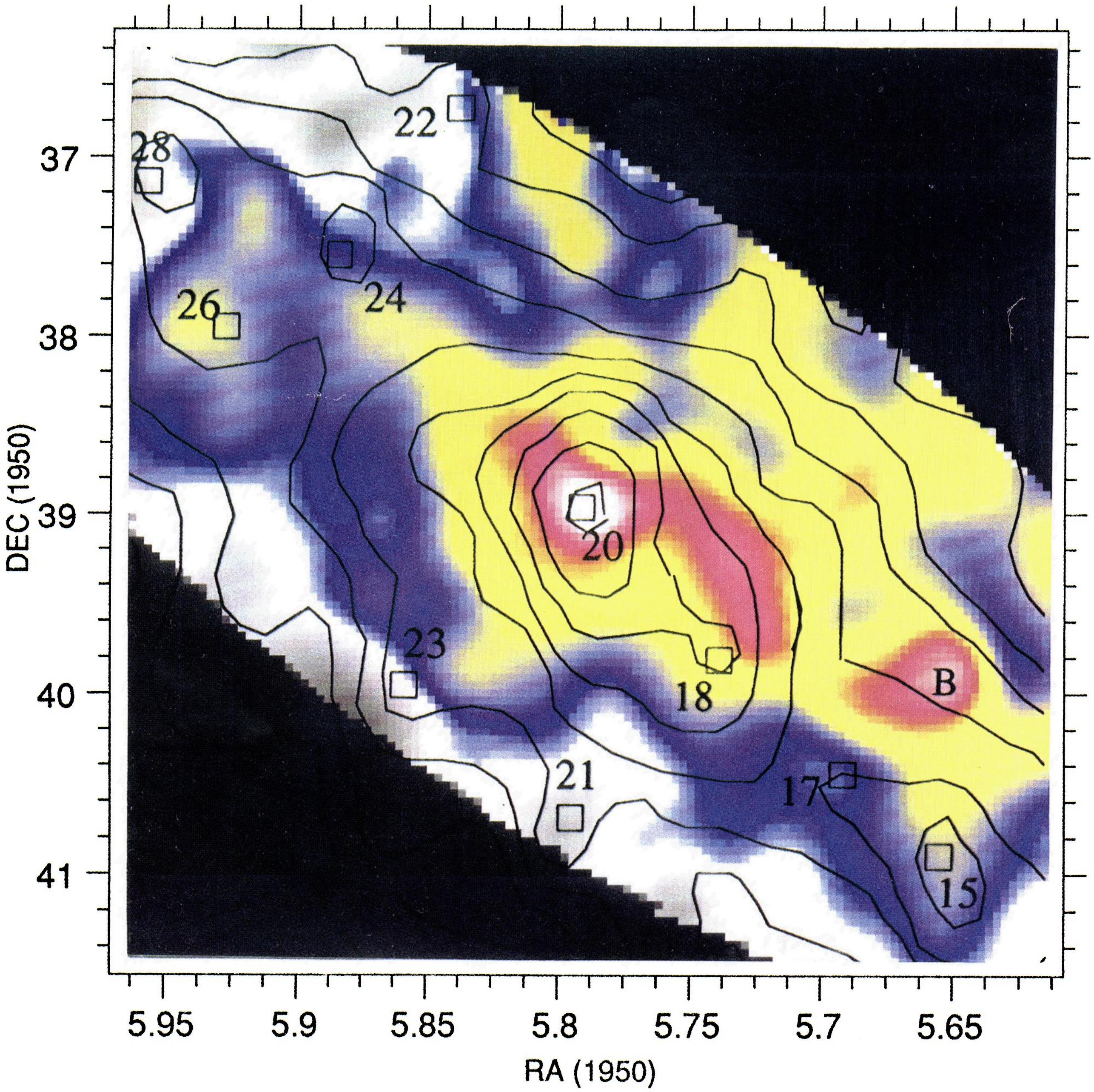

FIG. 4.—$J-K$ image of NGC 253. Overlaid are the 6 cm radio continuum contours and point sources as numbered by Antonucci & Ulvestaad (1988). The radio contours have a resolution (0"5 × 0"3) similar to our maps (0"5) and show an excellent overall correspondence to the extinction map. The bright point of high extinction in the center is the true galactic nucleus. The secondary bright peak marked "B" at position $\alpha = 00^h45^m05^s.65$, $\delta = -25°33'40".2$ is an artifact caused by the NIR peak's intrinsically different color, which spuriously increases the $J-K$ value in that area. The $J-K$ map has been shifted by ≈0"1 so that the extinction peak and the radio nucleus are precisely aligned.

SAMS et al. (see 430, L34)

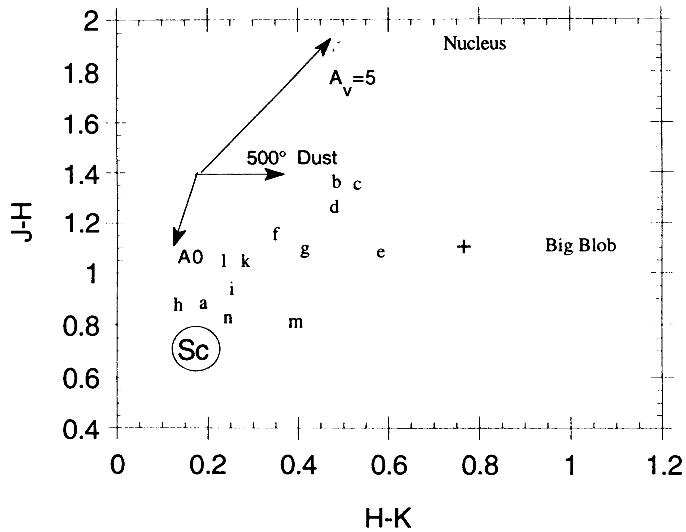

FIG. 5.—Color-color diagram of the "spots" in NGC 253. Also plotted are the shifting vectors due to (1) 5 mag of visual extinction caused by dust (Rieke & Lebofsky 1985); (2) the addition of 10% warm (500 K) dust (Glass & Moorwood 1985); and (3) the addition of 10% light from A0 stars (Doyen, Jopeph, & Wright 1991). The errors are derived from our absolute calibration errors, which would produce a systematic calibration error, shifting the entire plot, but affecting the *relative* positions of points very little. We estimate the relative positions are accurate to 0.05 mag. The circle marks typical nuclear colors of an Sc galaxy (Frogel 1988), and the cross marks the point for the entire nuclear region as measured by Scoville et al. (1985) within a 10″ aperture.

able in light of the fact that the observed structure is dominated by extinction and that the extinction at 2.2 μm and 10.8 μm differ by only a factor of 2 (Draine 1989). Furthermore, a visual inspection shows that the degraded-resolution K map has almost exactly the same shape as the 10.8 μm map. These considerations give us confidence that even though there is a possibility of systematic error resulting from the wavelength shift from 2.2 to 10 μm, such effects will be very small, considerably less than 0″.5. The weighted mean of the NIR peak derived from H and 10.8 μm derived measurements is then $\alpha = 00^h45^m05^s.67$, $\delta = -25°33'40''.1$, with an uncertainty of 1″.1. If we place the NIR intensity maximum at this position, it is 2″.28 distant from the radio nucleus at $\alpha = 00^h45^m05^s.79$, $\delta = -25°33'39''.0 \pm 0''.15$ (Turner & Ho 1985; Ulvestaad & Antonucci 1991), while the extinction peak's position falls only 0″.09 away from the radio nucleus. Thus we (1) verify with $>95\%$ statistical certainty that *the NIR intensity maximum is not the radio nucleus*, and (2) find that *the extinction peak is coincident with the radio nucleus*.

3.4. *Interpretation of the J − K Map*

To convert $J-K$ values to A_V, we apply $A_V = \beta(a_J - a_K)^{-1}(J-K-C_{JK})$, where $a_J = 0.282$ and $a_K = 0.112$ are the relative extinction at J and K compared to V (Rieke & Lebofsky 1985), $C_{JK} \approx 0.9$ is the intrinsic $J-K$ color of typical red supergiant–dominated Sc galaxies (Frogel 1985; Frogel 1988), and β is a correction factor (≥ 1) which depends on the extinction geometry. If the extinction is mingled with the emission (rather than lying between the observer and the source), the true extinction is greater than the measured extinction by a factor $\beta > 1$; if the emitter is entirely behind the absorber, $\beta = 1$. We estimated β for the high ($J-K \approx 2.9$, $A_V = 12\beta$) extinction regions by "dereddening" each pixel of the J-band map with an extinction of $-\beta a_J(a_J - a_K)^{-1}(J-K-C_{JK})$. When the J map in the region corresponding to the extinction peak appeared maximally smooth, β was $\approx 2 \pm 0.5$. Thus, high extinction values derived from the $J-K$ map probably have to be multiplied by ≈ 2 to compensate for the absorber/emitter geometry, which implies $A_V = 24 \pm 6$ at the extinction peak. In regions of lower measured extinction, β is close to 1, as we found by dereddening the entire J map (ignoring the region of the central extinction peak) and looking for maximal smoothness. The product is quite smooth (though not featureless) and has a power-law surface brightness profile of $B(r) \propto r^{-0.8 \pm 0.2}$ in the region $1'' < r < 5''$ (12–60 pc). Based on the $J-K$ map, we propose a structural model of the galaxy in which most of the brightness variations (and the gradient) measured in the NIR are due to the relatively smooth background light of the distributed red supergiants and K giants shining through a patchy dust/gas cloud with $A_V \approx 1$–5. The dense central extinction peak and its extensions are due to much denser (A_V reaching 20 or more), spatially compact, and clumpy material on the far side of the veil. The color gradient is consistent with our highly inclined view of NGC 253.

To convert the derived extinctions to molecular column densities, we adopt a standard dust/gas conversion constant, namely $N_H \equiv H_{H\,I} + 2N_{H_2} = 2.3 \times 10^{21} A_V$ (Jenkins & Savage 1974). The column densities then imply gas masses $M(H) = m_H \int_{source} N_H d\Omega = \beta 4.0 \times 10^2 D^2_{Mpc} \int_{source} A_V dS\, M_\odot$, where D_{Mpc} is the galactic distance in Mpc, m_H is the mass of hydrogen, Ω is solid angle, and S is the surface area in square arcseconds. The nuclear extinction (see Fig. 4) is $A_V = 12\beta = 24$. If we assume that the gas is spherically distributed, the implied molecular mass [for values of $D_{Mpc} = 2.5$, $\beta = 2$, $S = \pi(0''.25)^2$] is $\approx 1.1 \times 10^4\, M_\odot$ within the central 3 pc radius (0″.5 aperture) corresponding to the main part of the extinction peak. This very high density suggests the possibility that the radio nucleus itself is a massive source which has either gravitationally accreted a large halo or formed in a dense stellar/molecular cloud.

3.5. *Detection of Small Gas/Dust Extensions*

The $J-K$ map also shows narrow extensions leading out of the nucleus and along the major axis symmetrically in both directions for about 3″, or a total projected linear distance of ≈ 70 pc. They are relatively straight out to 3″ distance, where they form "arms" which bend sharply counterclockwise. This curvature is consistent with trailing spiral arms (Pence 1981) and suggests that these structures are either a "minispiral," or a "minibar" with the progenitors of spiral arms trailing from it. The extensions have typical $A_V \gtrsim 5$–10 ($N_H \approx 2 \times 10^{23}$ atoms cm^{-2}), or roughly a factor of 4 above the mean background. We consider this density enhancement, particularly given its geometry, to be very significant. After taking beam sizes into account, these column densities are in agreement with the mean value of 3.0×10^{22} H_2 cm^{-2} found in the molecular bar with ^{12}CO $J = 1 \rightarrow 0$ mapping in a 9″ × 5″ beam (Canzian, Mundy, & Scoville 1988). We compared the position angle of the two bar structures by convolving the CO beam with the $J-K$ image in which the NIR peak's color artifact was removed and the image values were quantized to 1 or 0 in order to mimic the "cloud counting" nature of optically thick CO measurements. We find a position angle of 57° ± 2, in agreement with the 58° ± 2 which we estimate for the central 10″ of the CO map. Based on these morphological and column density correlations, we suggest that our $J-K$ maps show the same structures as the CO map, but with much higher resolution. Whether these extensions are a "bar" or a "spiral" is difficult to determine, though at somewhat larger scales the position angle varies with radius (Pompea & Reike 1990), suggesting spiral arms instead of a bar structure.

3.6. *The Gas/Dust Extensions Trace Radio Emission*

The molecular material/dust map of Figure 4 is shown with the 6 cm radio contours and point sources (numbered according to Ulvestaad & Antonuuci 1991) in overlay. The radio resolution (0".5 × 0".3) closely matches ours and shows general agreement between the overall molecular and radio continuum distributions. The radio continuum has peaks near both ends of the gas/dust extensions where the extinction is particularly high ($A_V \approx 15$) and is also highly peaked near the nucleus. The correspondence is strong evidence that we have correctly interpreted the $J-K$ map as a tracer of molecular material. It also suggests that the primary heating source is diffuse, rather than pointlike (due, e.g., to a few giant H II regions). One potential heating source is a very large population of smaller H II regions. Other possibilities are large scale ionizing radiation fields permeating the entire cloud complex (Fabbiano 1988).

Although not all of the radio point sources in Figure 4 lie near an extinction peak, a significant fraction appear to be spatially correlated. Excluding the nucleus, four radio point sources (UA 15, 17, 18 and 26) lie within 0".25 of a local extinction peak. We count 15 such peaks within the ≈ 14 arcsec^2 area of the region, so the total area within 0".25 of a peak is $15\pi(0.25)^2 = 2.9$ arcsec^2; there is thus a random chance of $2.9/14 = 0.21$ that a source lies in such an area. Thus, the probability that four of nine sources lie as observed is given by the binomial distribution, $P_B(x, n, p) = P_B(4, 9, 0.21) = 0.075$, indicating a significant spatial correlation. If the radio sources were Type II supernovae and/or supernova remnants, such a correlation would be unlikely because the stars and gas clouds in a barred galaxy form two separate dynamical systems (Olson & Kwan 1990), causing newly formed massive stars to drift apart from their progenitor H II regions at approximately the rotation velocity. Rotation curves of NGC 253 show that $v \approx 0.4$ km s^{-1} pc^{-1} (Pence 1981; Canzian et al. 1988), so that sources at typical distances of 50 pc from the core velocities of ≈ 20 km s^{-1}, which would cover the observed spatial correlation length of 0".25/cos (78°) ≈ 17 pc in $\approx 8 \times 10^5$ yr, less than the lifetime of a massive star. Hence the radio sources are probably H II regions. Also supporting this hypothesis is the fact that the luminosity of Type II supernovae varies significantly with time, but the radio point sources in NGC 253 are relatively time invariant (Ulvestaad & Antonucci 1991).

We thank the observatory staff at ESO for their help with operating SHARP, A. Harris for helpful comments, and H. W. Paulsen for helping us keep our computers running.

REFERENCES

Antonucci, R. R. J., & Ulvestaad, J. S. 1988, ApJ, 330, L97
Canzian, B., Mundy, L. G., & Scoville, N. Z. 1988, ApJ, 333, 157
Christou, J. C. 1991, Exper. Astron., 2, 27
Combes, F., Gottesman, S. T., & Weliachew, L. 1977, A&A, 59, 181
Doyon, R., Jopeph, R. D., & Wright, G. S. 1991, in Astrophysics with Infrared Arrays, ed. R. Elston (Tuscon: ASP), 69
Draine, B. T. 1989, in Symp. on Infrared Spectroscopy in Astronomy (Salamanca, Spain: ESA), 93
Fabbiano, G. 1988, ApJ, 330, 672
Forbes, D. A., Ward, M. J., & DePoy, D. L. 1991, ApJ, 380, L63
Forbes, D. A., Ward, M. J., Rotaciuc, V., Blietz, M., Genzel, R., Drapatz, S., van der Werf, P. P., & Krabbe, A. 1993, ApJ, 406, L11
Frogel, J. A. 1985, ApJ, 298, 528
———. 1988, in Annual Review of Astronomy and Astrophysics, ed. G. Burbidge (Palo Alto: Annual Reviews), 51
Glass, I. S., & Moorwood, A. F. M. 1985, MNRAS, 214, 429
Harris, A. I., Hills, R. E., Stutzki, J., Graf, U. U., Russell, A. P. G., & Genzel, R. 1991, ApJ, 382, L75
Hofmann, R., Blietz, M., Duhoux, P., Eckart, A., Krabbe, A., & Rotaciuc, V. 1993, Progress in Telescope and Instrumentation Technologies, ed. M. H. Ulrich (Munich: ESO), 617
Jenkins, E. B., & Savage, D. B. 1974, ApJ, 187, 243
Koorneef, J. 1985, Infrared Standard Stars Table, European Southern Observatory, Revision 008
Lucy, L. B. 1974, AJ, 79, 745
Olson, K. M., & Kwan, J. 1990, ApJ, 349, 480
Pence, W. D. 1981, ApJ, 247, 473
Piña, R. K., Jones, B., & Puetter, R. C. 1992, ApJ, 401, L75
Pompea, S. M., & Reike, G. H. 1990, ApJ, 356, 416
Ribak, E. 1986, Journal of the Opt. Soc. Am. A, 3, 2069
Rieke, M. 1993, private comunication
Rieke, G. H., & Lebofsky, M. J. 1985, ApJ, 288, 618
Rieke, G. H., Lebofsky, M. J., & Walker, C. E. 1988, ApJ, 325, 679
Roddier, F. 1988, Phys. Rep., 170, 1
Scoville, N. Z., Soifer, B. T., Neugebauer, G., Young, J. S., Matthews, K., & Yerka, J. 1985, ApJ, 289, 129
Telesco, C. M., Dressel, L. L., & Wolsencroft, R. D. 1993, ApJ, 414, 120
Telesco, C. M., & Harper, D. A. 1980, ApJ, 235, 392
Turner, J. L., & Ho, P. T. P. 1985, ApJ, 299, L77
Ulvestaad, J. S., & Antonucci, R. R. J. 1991, AJ, 102, 875